Differential recruitment of opportunistic taxa leads to contrasting abilities in carbon processing by bathypelagic and surface microbial communities

Marta Sebastián[1,2], Irene Forn[1], Adrià Auladell[1], Markel Gómez-Letona[2], M. Montserrat Sala[1], Josep M. Gasol[1], Celia Marrasé[1]

[1] Departament de Biologia Marina i Oceanografia, Institut de Ciències del Mar, CSIC, 08003 Barcelona, Catalunya, Spain

[2] Instituto de Oceanografía y Cambio Global, IOCAG, Universidad de Las Palmas de Gran Canaria, ULPGC, 35214, Gran Canaria, Spain.

Running title: Contrasting patterns in carbon processing in the ocean

Correspondence to Dr Marta Sebastián, Departament de Biologia Marina i Oceanografia, Institut de Ciències del Mar, CSIC, 08003 Barcelona, Catalunya, Spain

Email: msebastian@icm.csic.es

The authors declare no conflict of interest

SIGNIFICANCE STATEMENT

Production of recalcitrant compounds is known to occur during organic matter processing by bacterioplankton, being an important component of the biological pump. Roughly twenty percent of the carbon produced in the sunlit ocean is exported to the deep ocean as dissolved compounds during winter overturn. Recent studies have shown that bathypelagic prokaryotes are metabolically versatile, but whether this versatility translates into a higher ability to process carbon has rarely been explored. To address this issue we performed a transplant experiment to compare the growth, activity and organic matter processing of surface and bathypelagic prokaryotes exposed to the same environmental conditions. We found that incubations with surface prokaryotes led to an accumulation of recalcitrant compounds, which did not occur with bathypelagic prokaryotes, suggesting they were able to process these compounds. These contrasting abilities to process DOM were attributed to the recruitment of a larger number of opportunistic taxa among the bathypelagic assemblages that likely resulted in a broader community capability of substrate utilization. The comparatively higher ability of bathypelagic prokaryotes to use recalcitrant DOC compounds would lead to a lower efficiency in the long-term sequestration of this carbon. Thus, future changes in the intensity of the overturning circulation due to climate change should have an impact on the persistence and fate of DOC in the ocean.

ABSTRACT

Different factors affect the way dissolved organic matter (DOM) is processed in the ocean water column, including environmental conditions and the functional capabilities

of the communities. Recent studies have shown that bathypelagic prokaryotes are metabolically flexible, but whether this versatility translates into a higher ability to process DOM has been barely explored. Here we performed a multifactorial transplant experiment to compare the growth, activity and changes in DOM quality in surface and bathypelagic waters inoculated with either surface or bathypelagic prokaryotic communities. The effect of nutrient additions to surface waters was also explored. Despite no differences in the cell abundance of surface and deep ocean prokaryotes were observed in any of the treatments, in surface waters with nutrients the heterotrophic production of surface prokaryotes rapidly decreased. Conversely, bathypelagic communities displayed a sustained production throughout the experiment. Incubations with surface prokaryotes always led to a significant accumulation of recalcitrant compounds, which did not occur with bathypelagic prokaryotes, suggesting they have a higher ability to process DOM. These contrasting abilities could be explained by the recruitment of a comparatively larger number of opportunistic taxa within the bathypelagic assemblages, which likely resulted in a broader community capability of substrate utilization.

INTRODUCTION

Microbes are the engines driving the earth's biochemical cycles (Falkowski *et al.*, 2008) and given that a large fraction of the earth's prokaryotes (i.e. Bacteria and Archaea) occur in the ocean (Whitman *et al.*, 1998; Bar-On *et al.*, 2018), marine prokaryotes play a pivotal role in ecosystem functioning. Although they have traditionally been considered a homogeneous black box, molecular studies and single-cell activity approaches have shown that marine prokaryotes are incredibly diverse, and highly heterogeneous in their levels of activity (Kirchman *et al.*, 2004; Sogin *et al.*, 2006; Alonso-Sáez and Gasol, 2007). These levels of activity are shaped by both the metabolic traits of the prokaryotes

and resource availability, which change drastically along the ocean water column: whereas the euphotic layer is rich in dissolved organic carbon and depleted in inorganic nutrients (e.g. Thingstad *et al.*, 1997), deep ocean waters are nutrient rich but limited by the availability of easily metabolizable organic carbon (e.g. Herndl and Reinthaler, 2013), which is mostly produced in the sunlit ocean.

As a consequence of the decrease in the availability of carbon, prokaryotic abundance and production decreases exponentially with depth (Arístegui *et al.*, 2009; Baltar *et al.*, 2009), and there is a drastic change in community composition and metabolic potential (DeLong *et al.*, 2006; Brown *et al.*, 2009; Sunagawa *et al.*, 2015). For example, bathypelagic prokaryotes harbor more genes devoted to polysaccharide degradation compared to their surface counterparts (DeLong *et al.*, 2006), which may explain the increase in cell specific enzymatic activities and specific uptake rates of polymeric substances towards deep waters (Baltar *et al.*, 2009; Boutrif *et al.*, 2011). In addition, the proportion of prokaryotic cells with high nucleic acids content (HNA cells) also increases with depth (Gasol *et al.*, 2009; Van Wambeke *et al.*, 2011), which might be indicative of larger genomes, in agreement with some genomic (Vezzi, 2005; Lauro and Bartlett, 2008), and global metagenomic observations (Acinas *et al.*, 2019). Large genomes may be the imprint of the pressure for metabolic versatility and an opportunistic life-style (Guieysse and Wuertz, 2012) to cope with the sporadic nature of carbon inputs (Smith *et al.*, 2018), a myriad of diluted organic compounds (Arrieta *et al.*, 2015), and the high proportion of recalcitrant substances (Hansell, 2013; Shen and Benner, 2020) typical of the bathypelagic realm. Indeed, bathypelagic communities have been previously shown to be very malleable in response to carbon starvation (Sebastián *et al.*, 2018), and to harbour opportunistic taxa that can swiftly respond to sudden inputs of organic carbon (Sebastián *et al.*, 2019). However, whether this metabolic flexibility translates into a

contrasting ability to process DOM has been barely explored (but see Boutrif *et al.*, 2011; Shen and Benner, 2018).

Here we performed a multifactorial transplant experiment to compare the growth potential, activity and changes in DOM quality in surface (5 m) and bathypelagic waters (2100 m depth) inoculated with either surface or bathypelagic communities (see Figure S1 for details on the experimental setup). Since growth and DOM utilization in the epipelagic is often limited by the availability of inorganic nutrients, the effect of nutrient additions to surface waters was explored as well. We also focused on the identity and dynamics of opportunistic taxa (i.e. the most responsive taxa) in the different conditions, to shed light onto the role of microbial structure on DOM processing by the surface and bathypelagic communities. Based on the presumably higher metabolic versatility of deep ocean communities, we hypothesized that under the same environmental conditions, bathypelagic prokaryotes would reach higher abundances, and would be more efficient in carbon utilization, than their surface counterparts.

RESULTS

Experimental initial conditions

As expected, surface seawater had initial inorganic nutrient concentrations one order of magnitude lower than bathypelagic waters (Table 1), but higher dissolved organic carbon (DOC) concentrations. The addition of inorganic nutrients to surface waters (SW + N treatment) resulted in nitrate and phosphate concentrations in the range of the values found in the bathypelagic waters (Table 1). On day 9 of the experiment a combination of carbon-based substances with different lability, including acetate,

glucose, terrestrial humic acids and amino acids (see Table S1), was added to half of the remaining bathypelagic waters (BW+C treatment), yielding DOC values close to the ones found in surface waters (Table 1).

Dynamics of prokaryotic cell abundance and heterotrophic production

The abundance of prokaryotic cells reached higher values in the surface water with inorganic nutrients (SW+N, ~$3 \cdot 10^5$ cells mL^{-1}) than in the SW and the BW treatments (~$1.4 \cdot 10^5$ cells mL^{-1}, Figure 1a), confirming that growth of both bathypelagic and surface communities in the SW treatment was limited by the availability of inorganic nutrients, whereas in the BW treatment the prokaryotes were limited by the availability of organic carbon. This carbon limitation was further proven by the addition of mixed carbon compounds to BW on day 9 of the experiment (see methods and Table S1), which caused a drastic increase in the cell abundance of both surface and bathypelagic communities, reaching values ca 3 -fold higher than in the SW+N treatment (~$8 \cdot 10^5$ cells mL^{-1}, Figure 1a). This large increase in abundance upon enrichment with some labile compounds as compared to the SW+N treatment, suggests that the DOC present in the surface waters was already partially recalcitrant. No significant differences in cell abundances were observed between surface and bathypelagic communities in any of the treatments (Figure 1a, Table 2).

Likewise, the cell size of surface and bathypelagic prokaryotes was also similar in the SW and BW treatments, and in the same range as the values observed for bathypelagic communities in the SW+N treatment (~0.1 μm^3, Figure 1b, Table 2). However, the size of surface cells in the SW+N treatment notably decreased after 8 days (Figure 1b), reaching 0.08 μm^3 at the end of the experiment. Flow cytometry cytograms showed that the change in cell size coincided with a sharp two-fold decrease in the number of high

nucleic acid (HNA) containing cells (Figure S2), and a shift of the community towards a dominance of low nucleic acid containing cells (LNA). Besides this shift, we also observed the appearance of a population of tiny cells (0.045 μm^3, i.e. microcells) in the surface communities of the SW+N treatment (Figure S2) that was not detected in the bathypelagic communities of this treatment, nor in any community in the other treatments (data not shown).

Leucine incorporation rates (as an estimate of heterotrophic prokaryotic production) of surface prokaryotes peaked on day 2 of the experiment in all treatments, then decreased notably from day 2 to day 3, and afterwards remained stable except for the SW+N treatment, where it continued to decrease until the end of the experiment (Figure 1c). The activity of bathypelagic prokaryotes in the SW+N treatment also increased in day 2, but unlike surface prokaryotes, bathypelagic cells maintained high levels of activity until day 10 of the experiment, when it slightly dropped (Figure 1c). The heterotrophic production of bathypelagic prokaryotes in the SW and BW treatments followed similar trends, increasing until day 10 of the experiment, but decreasing shortly afterwards, and not presenting the day 2 peak observed in surface prokaryotes. Analysis of the cumulative heterotrophic production throughout the experiment showed that it was higher with the bathypelagic prokaryotes than with the surface ones in all water treatments (Figure S3), although these differences were only significant for the SW+N and the BW+C treatments (Table 2).

Dynamics in community structure and diversity

We next explored the taxonomic composition of the communities in the different treatments and how it changed over time. Initial surface communities were dominated by SAR11 bacteria (53% of the reads), whereas bathypelagic communities had a high

181 proportion of Thaumarchaeota (38% of the reads, Figure 2). In order to remove predators,
182 we prefiltered the sample through a 0.8 μm pore size filter, and then collected the cells
183 onto a 0.2 μm filter. These cells were afterwards resuspended in particle free seawater,
184 counted by flow cytometry, and inoculated in equal amounts in each of the treatments
185 (see methods and Figure S1 for details). Detachment of cells from the filter is never 100%
186 efficient, and the prefiltration step may also remove large prokaryotic cells. Analysis of
187 the community structure after these steps unveiled that there was some change likely due
188 to the removal of large cells (Figure 2), indicated by the reduction in cyanobacterial
189 sequences from the surface communities, which are usually retained by the 0.8 μm filter
190 (Mestre *et al.*, 2017), and the enrichment in Thaumarchaeota, which are preferentially
191 found in the <0.8 μm size fraction (Salazar *et al.*, 2015), in the bathypelagic inoculum.
192 These manipulations resulted in a slight decrease in the Shannon diversity index of the
193 surface inoculum (from 3.1 to 2.6), but not in the bathypelagic inoculum (4.4 and 4.6 in
194 the initial community and the inoculum, respectively). However, a major change in
195 community composition was not observed. In contrast, there was a remarkable shift
196 within the next 40 h in the dominant taxa upon enclosure of the communities. Regardless
197 the water treatment (SW, SW+N, or BW), Gammaproteobacterial taxa dominated the
198 surface assemblages throughout the experiment (Figure 2, upper panel), and they also
199 represented a large proportion of the bathypelagic communities (Figure 2, lower panel).
200 Gammaproteobacteria in all treatments were mostly represented by two taxa (exact
201 amplicon sequence variants, 'ASV') of Alteromonadales, asv1 and asv2 (Figure S4, table
202 S2). These two taxa alone summed up ~90% of the surface assemblage sequences on day
203 2 of the experiment regardless the water treatment (Figure 2, upper panel, Table S2). The
204 contribution of these two taxa to the bathypelagic assemblages was also high but slightly
205 lower, accounting for ~60, ~70%, and 23% in the SW, SW+N, and BW treatment on day

206 2 of the experiment, respectively. Other gammaproteobacteria like Oceanospirillales also
207 accounted for a noteworthy fraction of the bathypelagic communities, representing
208 around 25% in the SW and SW+N treatments and ~50% in the BW treatment on day 2 of
209 the experiment, but they decreased in abundance with time. Conversely, Oceanospirillales
210 increased in abundance along the experiment in the surface assemblages when
211 transplanted into bathypelagic water (BW treatment), going from 3% of the community
212 on day 2 to ~22% on day 12. Nevertheless, upon carbon addition to the bathypelagic
213 water, the proportion of Oceanospirillales in the surface assemblages decreased again
214 (Figure 2, BW+C treatment).

215 Several alphaproteobacterial ASVs belonging to the Rhodobacterales order were
216 also major contributors to the bathypelagic communities in the last time points of the
217 experiment, particularly in the SW+N and the BW+C treatment, where they accounted
218 for 55% and 62% of the communities, respectively (Figure 2, Table S2). Similarly,
219 addition of dissolved organic carbon to the surface communities in bathypelagic waters
220 (BW+C treatment) resulted also in a notable increase in the contribution of
221 Rhodobacterales, represented by a single ASV (Table S2), which accounted for over 30
222 % of the community 2 days after the carbon input.

223 The reduction in size of surface-derived cells in the SW+N treatment (Figure 1),
224 together with the appearance of the population of tiny cells (Figure S2), was accompanied
225 with a swift change in the community composition from gammaproteobacterial
226 dominated to a larger contribution of Bacteroidetes (Flavobacteria) and
227 Alphaproteobacteria (Figure 2 upper panel, Table S2, Figure S4).

228 Over the course of the experiment bathypelagic communities displayed overall
229 higher diversity (Shannon index) and evenness than surface communities (Figure 3a).
230 Focusing only on the opportunistic taxa in each of the treatments, which we arbitrarily

defined as those ASVs that were initially rare but got recruited overtime and reached abundances over 5% of the community, we consistently found a higher number of opportunistic taxa in the bathypelagic assemblages in each of the water treatments compared to surface communities (Figure 3b).

Dynamics in hydrolytic activities

To investigate whether these taxonomic changes were accompanied by different physiological capabilities in surface and bathypelagic communities, we explored their enzymatic profiles in the different water treatments. We focused on the activities of α-glucosidase (AGase) and β-glucosidase (BGase), which are involved in the utilization of polysaccharides, leucyl aminopeptidase (LAPase), which degrades the proteinaceous components of DOM, and alkaline phosphatase (APase), involved in the hydrolysis of organic phosphoesters (Figure 4).

Contrary to the expectations of higher per cell hydrolytic rates in bathypelagic prokaryotes than in their surface counterparts, no major differences were observed between specific AGase and BGase activities of the surface and bathypelagic inocula within the different treatments (Figure 4), and both tended to increase towards the end of the experiment. The largest differences were found in the SW+N treatment, where the AGase and BGase activities of surface prokaryotes displayed a maximum on day 2, and decreased afterwards. Overall, both surface and bathypelagic communities showed lower specific AGase, and BGase rates in the BW treatment, probably reflecting lower availability of substrates (Figure 4). Surface prokaryotes displayed higher specific LAPase activity values than their bathypelagic counterparts in the surface water treatments (SW and SW+N) within the first days of the experiment (Figure 4). In the BW treatments, both communities showed similar trends in specific LAPase activities, with

low values throughout the experiment and a maximum at the last time-point. Upon the addition of the mixed sources of organic C to the bathypelagic water there was a remarkable increase in total hydrolytic activities (Figure S5), which reached similar values in both the surface and bathypelagic communities. However, the per cell AGase, BGase and LAPase activities in the BW+C treatment were within the range of those observed in the rest of the treatments, indicating that there was not an enhancement of the cell-specific activities (Figure 4).

In contrast, APase activities showed clear differences between both communities in some of the treatments, particularly in surface waters (SW). Addition of inorganic nutrients in the SW+N treatment led to a repression of the APase enzymes, and per cell specific activities were very low and constant for both communities in this treatment (Figure 4). Specific APase activities were higher in the BW treatment than in the SW+N treatment, particularly for the surface assemblage (Figure 4, third panel). Addition of organic carbon to the BW resulted in the decrease of APase specific activities (Figure 4, fourth panel).

DOM processing by surface and bathypelagic communities

To investigate if surface and bathypelagic communities had different abilities at DOM processing, we looked at changes in DOM quality by exploring the optical properties of chromophoric DOM (CDOM) and, in particular, of its fluorescent fraction (FDOM) (see methods for further details). We first focused on the dynamics of fluorescent humic-like (peak C in FDOM) and protein-like (peak T in FDOM) substances (Coble, 1996) and their ratio (peak C/peak T), which is an indication of the amount of recalcitrant versus labile fluorescent material (Baker *et al.*, 2008). Initial values in Peak C where higher in BW than in surface waters (SW, SW+N, Figure 5a). However, peak C

281 increased in all treatments inoculated with surface prokaryotes, reaching values
282 significantly higher than those obtained with bathypelagic prokaryotes in all treatments
283 at the end of the experiment (Wilcoxon test, see Table S3 for the p-values). In contrast,
284 values of peak T were only significantly higher at the final time point of the experiment
285 in the SW and BW+C treatments inoculated with the bathypelagic prokaryotes (Wilcoxon
286 test, Table S3). Peak T considerably increased upon carbon addition to the BW treatment
287 (Figure 5a, right panel), but it rapidly decreased afterwards, indicating that there was a
288 fast consumption of the labile compounds by both the surface and bathypelagic
289 prokaryotes.

290 The proportion of humic-like versus labile material (peak C/peak T ratio) in the SW
291 treatment was rather constant for both the surface and bathypelagic communities,
292 although it reached significantly higher values with the surface prokaryotes at the end of
293 the experiment (Figure 5a, Wilcoxon test, Table S3). In the SW+N treatment both surface
294 and bathypelagic communities showed opposite trends: whereas the C/T ratio
295 significantly increased with the surface prokaryotes, pointing to a net production of humic
296 substances, the C/T ratio decreased with the bathypelagic prokaryotes. In the BW
297 treatment, the C/T ratio values were high at the beginning of the experiment, but later
298 decreased along the experiment, being this decrease more evident with the bathypelagic
299 inocula than with the surface one (Figure 5a). The organic carbon addition resulted in low
300 C/T ratios due to the large proportion of amino acids added (treatment BW+C, Figure 5a,
301 right panel). At the end of the experiment the C/T ratio of this treatment increased, but
302 this increase was significantly higher with the surface prokaryotes than with the
303 bathypelagic prokaryotes, as in the rest of the treatments (Wilcoxon test, Table S3).

304 The spectral slope of the chromophoric DOM in the 275-295 nm wavelength range
305 is also an indicator of the quality of the organic matter, with lower values indicating an

306 increase in aromaticity and/or higher molecular weight (Helms *et al.*, 2008). There was a
307 notable decrease (30%) in this spectral slope from the beginning to the end of the
308 experiment in all the treatments inoculated with surface prokaryotes (Figure 5b), whereas
309 the decrease was much lower (<5%) in those treatments inoculated with bathypelagic
310 prokaryotes, suggesting that surface prokaryotes produced aromatic compounds during
311 the experiment.
312

313 **DISCUSSION**

314 Many factors affect prokaryotic growth and DOM processing in the ocean,
315 including environmental conditions, the metabolic potential of the prokaryotes, and the
316 quality and quantity of the available resources (Jiao *et al.*, 2010; Arrieta *et al.*, 2015;
317 Carlson and Hansell, 2015), and these factors are known to change drastically along the
318 water column. Our experimental approach enabled us to compare surface and
319 bathypelagic communities under the same environmental conditions, thus focusing only
320 on the effect of the community structure and metabolic capabilities of surface and
321 bathypelagic prokaryotes in community growth and DOM processing.

322 The lack of significant differences in the maximum cell abundance reached by
323 surface and bathypelagic communities within each of the treatments was surprising given
324 the difference in community structure of the starting communities, and suggests that the
325 environmental conditions, and not the genetic potential of the community, is the factor
326 controlling the biomass yield. This contrasts with a previous study that did find higher
327 biomass yields when surface waters were inoculated with upper mesopelagic
328 communities (250 m) than with surface ones (Carlson et al 2004), although noticeably, in
329 that study the starting cell abundance in the mesopelagic inocula was much lower than
330 the surface one, allowing for a higher prokaryotic growth.

Addition of inorganic nutrients to surface waters stimulated the growth of both the surface and bathypelagic prokaryotic communities (Figure 1, SW+N treatment), as frequently observed in the Mediterranean (Pinhassi *et al.*, 2006) and other oligotrophic regions (Cotner *et al.*, 1997; Mills *et al.*, 2008). However, despite both communities reached similar abundance values, after 8 days surface communities experienced a drastic change in cell size concomitantly with the appearance of a population of microcells (Figure S2). This suggests that by that time a fraction of the surface prokaryotes had become carbon-limited, as miniaturization and/or fragmentation are well-described phenotypic characteristics of growth-arrested cells upon carbon starvation (Novitsky and Morita, 1976, 1977; MacDonell and Hood, 1982; Kolter, 1993). Since this phenotypic response is common to several groups of Gammaproteobacteria (MacDonell and Hood, 1982), we hypothesize that the population of tiny cells originated from the Alteromonadales taxa that dominated the surface communities. 16S rDNA sequencing cannot differentiate between living, dormant or dead cells, so we used Catalyzed Reporter Deposition Fluorescent In situ Hybridization (CARDFISH) to test this hypothesis, by quantifying the percentage of gammaproteobacterial cells that contained intact ribosomes (or enough ribosomes to be detected) at the end of the experiment (see supplementary methods). While the contribution of *Alteromonas* to the 16S-based surface community in the SW+N treatment was over 60% at the final time point (Figure 2), Gammaproteobacterial cells only represented 25% of the cells (Figure S6). Furthermore, 50% of the surface community in this treatment did not have enough ribosomes to be detected at the end of the experiment, whereas in the bathypelagic community cells not detected by CARD-FISH represented only 10% (Figure S6). This suggest that under non-limiting conditions for growth (i.e. with enough organic carbon and nutrients) *Alteromonas* in the surface communities became dormant or dead when the organic

356 resources they could exploit became limiting. Consistently with our results, Pedler et al.
357 (2014) experimentally demonstrated that a single species of *Alteromonas* could consume
358 all labile carbon present in surface waters in only three days, but was not able to further
359 exploit the remaining carbon. The steady decrease in the heterotrophic production of
360 surface communities after day 4 of the experiment, as opposed to the sustained production
361 that bathypelagic prokaryotes displayed until the end of the experiment, support the view
362 that surface prokaryotes became carbon limited in the SW+N treatment due to the
363 exhaustion of easily metabolizable carbon. These results point to different abilities in
364 resource utilization by the surface and bathypelagic communities.

365 The higher diversity and evenness observed in the bathypelagic communities
366 compared to the surface ones (Figure 3) are consistent with previous findings in the
367 Mediterranean and elsewhere (e.g. Pommier *et al.*, 2010; Agogué *et al.*, 2011; Ghiglione
368 *et al.*, 2012), although there are also some reports of decreasing values with depth (Brown
369 *et al.*, 2009). *Alteromonas* were the major contributors to both surface and bathypelagic
370 communities in all water treatments as often observed in amended or unamended
371 microcosms with surface and deep ocean communities (Eilers *et al.*, 2000; Schäfer *et al.*,
372 2000; McCarren *et al.*, 2010; Nelson and Carlson, 2012; Sebastián *et al.*, 2018).
373 *Alteromonas* display the highest growth rates within marine microbial communities and
374 are generally top-down controlled (Ferrera *et al.*, 2011; Sánchez *et al.*, 2017), and as
375 grazers were removed during the experimental setup, the dominance of this genus was
376 somehow expected. *Alteromonas* comprises copiotrophic taxa that have a preference for
377 a particle associated life-style (Acinas *et al.*, 1999; Mestre *et al.*, 2018), and may have a
378 cosmopolitan distribution throughout the water column using these particles as dispersion
379 drivers (Mestre *et al.*, 2018). The fact that we found the same two *Alteromonas* ASVs
380 blooming in both the surface and bathypelagic water treatments (Table S2), might suggest

that these ASV were indeed cosmopolitan taxa. However, 16S rRNA gene sequencing often has poor resolution at defining taxa and may hide different ecotypes within each ASV (VanInsberghe *et al.*, 2020), so it is also possible that our two ASVs represent different species in surface and bathypelagic communities. In order to further explore this, we aligned the V4-V5 region amplified sequences of our two *Alteromonas* ASVs with other known sequences of *Alteromonas* species and analyzed their sequence identity (Figure S7, see methods for further information). We found that *Alteromonas* asv1, our dominant ASV, was 100% identical to sixteen different *Alteromonas* species, and asv2 was 100% identical to four other *Alteromonas* species. This means that we cannot rule out that the ASVs detected in the bathypelagic assemblages represented different species than the surface ones, which may explain why we observed miniaturization in the surface but not in the bathypelagic communities. Nevertheless, other studies have described cosmopolitan distribution of some *Alteromonas* taxa in both sunlit and deep ocean waters (Lopez-Lopez *et al.*, 2005; Ivars-Martinez *et al.*, 2008; López-Pérez *et al.*, 2012). In any case, regardless whether the two ASVs were cosmopolitan taxa or distinct ecotypes, the fact that *Alteromonas* bloomed in all the treatments suggests this genus is responsible for the rapid utilization of a large fraction of the labile carbon throughout the water column, and not only in surface waters (Pedler *et al.*, 2014).

Besides the two dominant *Alteromonas* ASVs, bathypelagic communities harbored several opportunistic ASVs belonging to Rhodobacterales (Figure S4, Table S2). This group of bacteria are also copiotrophs with a preference for a particle associated lifestyle (Li *et al.*, 2015; Mestre *et al.*, 2018; Gómez-Consarnau *et al.*, 2019) and may reach relatively high abundances in the bathypelagic realm (Salazar *et al.*, 2016; Mestre *et al.*, 2018). The increase in bathypelagic Rhodobacterales in late time points of the experiment and the sustained heterotrophic production throughout the experiment, suggest they were

406 able to exploit the remaining DOM compounds after *Alteromonas* had exhausted the most
407 labile DOM, pointing to a succession of specialized opportunistic taxa. Thus,
408 Rhodobacterales outcompeted *Alteromonas*, but perhaps the later could thrive on by-
409 products of Rhodobacterales metabolism, which could also be a plausible explanation of
410 why we did not observe any cell miniaturization in the bathypelagic communities in the
411 SW+N treatment.

412 Analyses of the optical properties (fluorescence and absorbance) of DOM provided
413 insight into the composition of dissolved organic matter and its processing. Initial values
414 of peak C (humic-like material) and C/T ratio (proportion of humic versus labile material,
415 see methods) were higher in bathypelagic than in surface waters (SW, SW+N, Figure 5a),
416 in agreement with the largely recalcitrant nature of bathypelagic DOM (Hansell, 2013;
417 Catalá *et al.*, 2016; Martínez-Pérez *et al.*, 2017).

418 Over the course of the experiment, in all treatments inoculated with surface
419 communities we consistently observed a significant increase in the proportion of
420 recalcitrant compounds (C/T ratio) and a net decrease in the $S_{275–295}$ spectral slope of
421 CDOM (Figure 5), which can be associated with a raise in DOM molecular weight or
422 aromaticity (Helms *et al.*, 2008). Conversely, this increase in recalcitrant compounds did
423 not occur in the treatments inoculated with the bathypelagic communities. Production of
424 recalcitrant compounds that persist during long-term incubations is known to occur
425 during organic matter processing by bacterioplankton (Brophy and Carlson, 1989; Ogawa
426 *et al.*, 2001; Ortega-Retuerta *et al.*, 2009; Romera-Castillo *et al.*, 2011; Osterholz *et al.*,
427 2015). The fact that these compounds did not accumulate with the bathypelagic
428 assemblages suggests that the consumption of these compounds was greater than their
429 production, indicating that bathypelagic prokaryotes were more efficient at the processing
430 of recalcitrant compounds than their surface counterparts. Similarly, Carlson et al. (2004)

found higher DOC drawdown with upper mesopelagic communities (250 m) than with surface ones. In contrast, no differences in DOC drawdown were observed between surface and bathypelagic communities subjected to additions of recalcitrant and plankton-derived DOC (Shen and Benner, 2020). Despite we could not estimate net DOC utilization rates in our study due to the unfortunate contamination of the DOC samples, our observations imply that there is a fundamental difference in the way DOC is processed by bathypelagic and surface prokaryotes.

The lack of net production of recalcitrant compounds by bathypelagic prokaryotes may result counterintuitive with the prevalent view of higher proportion of recalcitrant compounds in the bathypelagic ocean (Hansell, 2013; Catalá *et al.*, 2016; Martínez-Pérez *et al.*, 2017) and the positive relationship usually found between FDOM and apparent oxygen utilization (which integrates respiratory processes) in deep waters (Yamashita and Tanoue, 2008; Jørgensen *et al.*, 2011; De La Fuente *et al.*, 2014; Catalá *et al.*, 2015). However, it is probably a matter of the temporal scale of our experiment, and recalcitrant compounds would likely end up accumulating also with the bathypelagic prokaryotes once all the compounds they could exploit had been consumed. In fact, previous experiments with bathypelagic prokaryotes have shown both production and consumption of recalcitrant compounds over time (Aparicio *et al.*, 2015), and it has been recently shown that both production and removal of recalcitrant DOC occurs in the deep ocean (Romera-Castillo *et al.*, 2019).

It could be assumed that the bathypelagic prokaryotes are more efficient at hydrolyzing DOC compounds than surface ones given the typical higher per cell enzymatic activities found in the deep ocean (Baltar *et al.*, 2009). However, we did not observe striking differences between surface and bathypelagic communities in the specific enzymatic rates, except for APase activities, which are involved in the hydrolysis

of organic phosphorus compounds. APase induction is mostly controlled by phosphate availability and the internal phosphorus (P) reserves, and it is induced when prokaryotes do not have enough inorganic phosphorus to meet their demands (Hoppe, 2003). The large difference in activities between surface and bathypelagic prokaryotes in the SW treatment indicates that surface prokaryotes, unlike bathypelagic prokaryotes, did not have internal P reserves and relied on alkaline phosphatases to hydrolyze organic P compounds to obtain assimilable P. This is supported by the observation that in the phosphate-rich SW+N treatment the APase values for both communities were similar (Figure 4). Higher values in the BW treatment than in the SW+N treatment are in agreement with findings of high specific APase activities in deep waters (Hoppe and Ullrich, 1999; Baltar *et al.*, 2009), which have been hypothesized to be related to the acquisition of carbon from dissolved organic phosphorus compounds (Hoppe and Ullrich, 1999). Indeed, the fact that we observed a decrease in APase activities upon carbon addition in the BW+C treatment (Figure 4, fourth panel) is consistent with the hypothesis that APases are used to obtain the carbon moiety of the organic phosphorus compounds in deep waters. Despite these differences in APase activities, the per-cell activity rates of enzymes involved in carbohydrate hydrolysis (AGase and BGase) were quite similar among bathypelagic and surface prokaryotes. Thus, overall the main difference we observed between surface and bathypelagic communities was that bathypelagic assemblages were more diverse and seemed to harbor a higher proportion of resourceful taxa (Figure 3), because the number of ASVs accounting for more than 5% each experimental time-point was always higher in the bathypelagic assemblages. It is thus likely that the combined effort of these resourceful taxa resulted in the exploitation of a wider spectra of DOM compounds. Notably, however, the utilization of these compounds may imply a higher energetic cost, because bathypelagic prokaryotes generally displayed

481 higher cumulative leucine incorporation than the surface ones, while prokaryotic
482 biomasses were similar (Table 2, Figure S3), an indication that this extra leucine is likely
483 catabolized for energy production (see del Giorgio *et al.*, 2011).

484 It is important to point out that the bathypelagic prokaryotes experienced a dramatic
485 change in conditions during water collection, particularly in pressure, and it is possible
486 that some pressure-sensitive prokaryotes died during the process of water recovery.
487 Increasing efforts are being directed towards the development of devices and approaches
488 that take into account the effect of hydrostatic pressure on the activity of bathypelagic
489 communities (Grossart and Gust, 2009; Edgcomb *et al.*, 2016; Cario *et al.*, 2019; Garel
490 *et al.*, 2019). However, experiments using these devices have shown that respiration and
491 activity is usually lower under atmospheric pressure than under high in situ pressure
492 (Tamburini, Boutrif, *et al.*, 2013; Garel *et al.*, 2019), implying that bathypelagic
493 prokaryotes could even be more efficient at DOM processing than what we have observed
494 here.

495 Our findings further support the idea that bathypelagic communities are extremely
496 versatile, as hinted by experimental (Boutrif *et al.*, 2011; Sebastián *et al.*, 2018, 2019),
497 genomic and metagenomic evidence (Vezzi, 2005; DeLong *et al.*, 2006; Acinas *et al.*,
498 2019), and can use compounds that are resistant to surface communities. Although it had
499 already been hypothesized that organic compounds that accumulate in the surface ocean
500 may serve as substrates for mesopelagic populations (Carlson *et al.*, 2004, 2011), our
501 work indicates that this may also be the case for bathypelagic prokaryotes. DOC is
502 exported to deep layers of the ocean through winter mixing, or during processes of deep-
503 water formation (Carlson *et al.*, 1994; Hansell and Carlson, 2001; Hopkinson and Vallino,
504 2005; Treusch *et al.*, 2009; Santinelli, 2015), being this export an important component
505 of the biological pump (Copin-Montégut and Avril, 1993; Hopkinson and Vallino, 2005;

Carlson *et al.*, 2011). In the NW Mediterranean, where the water for this experiment was collected, deep water formation occurs episodically and seasonally as a consequence of both dense shelf water cascading and open-sea convection, which may last several days (Béranger *et al.*, 2009). During this process, fresh organic matter is conveyed to deep ocean prokaryotic communities (Tamburini, Canals, *et al.*, 2013; Severin *et al.*, 2016), and sometimes the convection is so intense that resident deep water is completely replaced by newly formed deep water, yielding high DOC concentrations in the bathypelagic (Luna *et al.*, 2016). The comparatively higher ability of bathypelagic prokaryotes to use these DOC compounds points to a lower efficiency in the long-term sequestration of this exported carbon, which has implications for the global carbon cycle. Thus, future changes in the intensity of the overturning circulation due to climate change should have an impact on the persistence and fate of DOC in the ocean.

METHODS

Experimental set up

Water was collected on September 29th 2014 from the surface (5 m, ~100 L) and the bathypelagic (2100 m, ~60 L) of the Northwestern Mediterranean Sea (40º 38' 31.01''N, 2º 51' 1.6''W) during the MIFASOL-I cruise on board the R/V García del Cid. The water was taken at night the last day of the cruise before steaming back to harbour, filtered through a 200 μm mesh to remove large zooplankton and poured into different thoroughly acid-rinsed 20-L containers. Once in the laboratory, 18 L of water from each depth were gently filtered through a 0.8 μm pore size filter, and prokaryotic cells were collected onto a 0.2 μm polycarbonate filter to generate the prokaryotic inocula for the transplant experiments (see Figure S1 for details on the experimental set-up). The remaining water was 0.2 μm filtered to produce cell-free water for the different treatments, described below. Filtration was carried out gently to avoid disruption of cells that could release carbon compounds. Prior to filtering, 3 L of miliQ water were flushed through the system to minimize organic carbon contamination. Cells collected from the surface and bathypelagic were resuspended in 0.9 L of their corresponding 0.2 μm filtered seawater and prokaryotic abundance was quantified through flow cytometry and then diluted so that the starting inoculum was the same in all treatments ($5x10^4$ cells mL^{-1}, that represented 1.1 ± 0.02 μg C L^{-1} (average ± SE)). Four 20-L carboys containing 0.2 μm filtered surface seawater ('SW') and two 20-L carboys containing 0.2 μm filtered bathypelagic seawater ('BW') were prepared and inoculated with either surface (Sp) or bathypelagic (Bp) prokaryotic cells. Inorganic nutrients were then added to one of the SW carboys containing Sp and to another containing Bp to yield the SW+N treatments. The amount of inorganic nutrients added was enough to reach similar concentrations to

547 the ones usually found in the Mediterranean bathypelagic (see Table 1). After prokaryotic
548 cells and inorganic nutrients (when appropriate) had been added to the 20-L containers,
549 that volume was divided into two replicates and deposited in the 10-L containers. The
550 experiment was performed in the dark, with surface water treatments being kept at room
551 temperature (~20ºC) and bathypelagic water kept at 16ºC, which is ca. 3 degrees higher
552 than the usual Mediterranean bathypelagic temperature. On day 9 of the experiment, the
553 remaining water volume in the BW treatment was divided in half into two containers and
554 carbon (mixed sources, including glucose, acetate, terrestrial humic acids and amino
555 acids, see Table S1 for details) added to one of the containers. This treatment was named
556 BW+C, and aimed to explore the short-term response of the communities developing in
557 bathypelagic water to a sudden input of carbon of different levels of lability, with total
558 DOC concentration values closer to the ones observed in the surface waters (Table 1).
559
560 *Total organic carbon*
561 Ten-mL water samples were collected in precombusted (450 °C, 24 h) glass
562 ampoules. After adding 50 µL of 25% H_3PO_4 to acidify at pH < 2, the ampoules were
563 heat-sealed and stored in the dark at 4°C until analysis. TOC concentrations were
564 quantified with a Shimadzu TOC-LCSV organic C/N analyzer. Between 3 and 5
565 injections of 150 µL per replicate were performed. The final organic carbon concentration
566 in each sample was calculated by subtracting a Milli-Q blank and dividing by the slope
567 of daily-made standard curves created using potassium hydrogen phthalate. Reference
568 samples of the Material Reference Certificate (MRC Batch-13 Lot // 08-13, Hansell
569 Laboratory. University of Miami, RSMAS) were used daily for quality control. Only data
570 on the initial TOC samples that were measured immediately after collection are available,

because many of the samples got contaminated during storage due to a defective batch in the glass vials where the samples were collected.

Inorganic nutrients

Samples for inorganic nutrients (10 mL) were kept frozen at −20°C until analysis, which was performed using a CFA Bran + Luebbe autoanalyser following the methods described by Hansen and Koroleff, (2007).

Flow cytometry analyses

Prokaryotic cell abundance was estimated by flow cytometry as described elsewhere (Gasol and Morán, 2015). The average cell biovolume was estimated using the relative FL1 signal following Gasol and del Giorgio (2000) and an in-house calibration between Syto13 and SybrGreen. This calibration was performed by staining cells with both dyes and correlating the fluorescence signal (standardized to the fluorescent signal of the same plastic beads) of both dyes.

The carbon content of the prokaryotic cells was computed using the allometric relationship of Norland *et al.*, (1993): pg C $cell^{-1}$ = 0.12 pg (μm^3 $cell^{-1}$)$^{0.7}$, and the biomass by multiplying the carbon content by the abundance of cells.

Prokaryotic heterotrophic production

Prokaryotic heterotrophic production was estimated from the incorporation of tritium-labelled leucine, which measures protein synthesis (Kirchman *et al.*, 1985). Four replicates of 1.2 ml and two trichloroacetic acid (TCA)-killed controls were incubated with ^{3}H-Leucine at a final concentration of 40 nM. Although 40nM may seem high for oligotrophic regions and could stimulate production, previous experiments showed this

596 concentration is saturating and was chosen to estimate potential activity in order to
597 facilitate comparison between treatments. Incubation was performed in the dark at *in situ*
598 temperature for 4 h and stopped with 5% TCA, final concentration. The samples were
599 then kept frozen at -20°C until processing, following Smith and Azam, (1992). Briefly,
600 samples were thawed and centrifuged for 10 min at 12000 x g. Supernatant was removed
601 and 1mL TCA 5% was added to the tubes and mixed by vortexing. Samples were again
602 centrifuged for 10 min at 12000 x g, the supernatant aspirated, and 1mL of liquid
603 scintillation cocktail (Optimal HiSafe) was added to the each of the tubes. The tubes were
604 then placed into 20-mL scintillation vials, stored in the dark for at least 24h, and radio-
605 assayed on a Beckman scintillation counter. Conversion of leucine to carbon units was
606 done with the theoretical factor 1.5 kg C mol Leu^{-1} (Simon and Azam, 1989).
607
608 *Enzymatic activities*

609 Leu-aminopeptidase (LAPase), α-glucosidase (AGase), β-glucosidase (BGase),
610 and alkaline phosphatase (APase) activities, were estimated using the following
611 fluorogenic substrates: L-leucine-7-amino-4-methylcoumarin, 4-methylumbelliferyl α -
612 D-glucoside, 4-methylumbelliferyl β-D-glucoside, and 4-methylumbelliferyl phosphate,
613 respectively (all purchased at Sigma-Aldrich) following the method developed by Hoppe,
614 (1983). Assays were performed as described in Sala *et al.*, (2016). Briefly, each sample
615 (350 µl) was pipetted in quadriplicate into 96 black well plates, and substrates were added
616 to obtain a final concentration of 125 µM. This concentration has been found to be
617 saturating in previous experiments and was thus chosen to estimate potential activities, to
618 facilitate comparison among treatments. The fluorescence of the 96 well plates was
619 measured with a Tecan Infinite 200 microplate reader at 365 nm excitation and 450 nm
620 emission wavelengths, at the beginning and after 5 hours of incubation at in situ

621 temperature conditions. Activity was derived from the increase in fluorescence in each
622 well over time, using a standard curve prepared with the fluorophores 4-
623 methylumbelliferone (MUF) or 4-methylcoumarinyl-7-amide 4 (Sigma-Aldrich).

624

625 *Optical Characterization of DOM*

626 The optical properties of colored dissolved matter (CDOM) and of its fluorescent
627 fraction (FDOM) provide information about the origin and lability of DOM. We inspected
628 these properties to evaluate possible changes in DOM lability in the different treatments.
629 Samples for FDOM characterization were collected on day 0, day 9 and day 13 of
630 the experiment. FDOM was measured using a Perkin Elmer LS55 luminescence
631 spectrometer provided with a xenon discharge lamp equivalent to 20 kW for an 8-μs
632 duration. A red sensitive R928 photodiodemultiplier operated as a reference detector.
633 Samples were measured in quadruplicate in a 1 cm acid-cleaned quartz cell at a constant
634 room temperature. Quartz cells were rinsed with sample water before analyses. We
635 focused on the detection of humic-like substances that fluoresce at 440 nm when excited
636 at 340 nm (peak-C, Coble, 1996), which are recalcitrant compounds produced in situ by
637 marine microorganisms (Castillo *et al.*, 2010; Romera-Castillo *et al.*, 2011; Jørgensen *et*
638 *al.*, 2014) and have been related to respiration processes in the ocean (De La Fuente *et*
639 *al.*, 2014). We also looked at peak-T (Coble, 1996), which relates to protein like
640 substances with Excitation/Emission wavelengths of 280 nm/350 nm and is used as a
641 tracer of biologically labile DOM (Yamashita and Tanoue, 2003). The humic-like vs
642 protein-like ratio (peak-C/peak-T) was then used as a proxy of DOM lability. Fluorescent
643 data was normalized to Raman units (R.U.) according to Lawaetz and Stedmon, (2009).
644 Samples for CDOM were taken at the beginning and the end of the experiment.
645 CDOM absorption was measured in a Varian Cary spectrophotometer equipped with a 10

646 cm quartz cell. The spectra were collected between 250 and 750 nm at constant room
647 temperature using Milli-Q water as blank. The absorption spectra was calculated as in
648 Romera-Castillo *et al.*, (2013). Following Helms et al. (2008), CDOM spectral slopes
649 were obtained in the 275-295 nm wavelength range ($S_{275–295}$) using liner regressions of
650 the natural log-transformed absorption spectra. This range was selected because it
651 provides information on the molecular weight and the aromaticity of the substances, with
652 lower slopes as the molecular weight and the aromaticity increase (Helms *et al.*, 2008).

653

654 *Nucleic acid extraction*

655 Samples for nucleic acid extraction (0.5-1 L) were filtered through 47-mm 0.2 μm
656 polycarbonate filters with a peristaltic pump, and filters were stored frozen until
657 extraction. Total nucleic acids were extracted using the PowerWater DNA isolation Kit
658 (MO BIO Laboratories, Carlsbad, CA) following the manufacturer instructions. DNA
659 was quantified using a Qubit fluorometer assay (Life Technologies, Paisley, UK). The
660 V4-V5 region of the 16S rRNA gene was amplified with the primers 515F-Y and 926R
661 (Parada et al. 2016) and sequenced in an Illumina MiSeq platform using 2x250bp paired-
662 end approach at the Research and Testing Laboratory facility (Lubbock, Texas, USA;
663 http://www.researchandtesting.com).

664 *Data analyses*

665 Computing analyses were run at the Marine Bioinformatics Service of the Institut de
666 Ciències del Mar (ICM-CSIC) in Barcelona. Primers and spurious sequences were
667 trimmed using cutadapt (Martin, 2011) using the following parameters: --discard-
668 untrimmed --minimum-length=32. DADA2 v1.8 was used to differentiate exact sequence
669 variants (Callahan *et al.*, 2016). DADA2 resolves ASVs (amplicon sequence variants) by
670 modelling the errors in Illumina-sequenced amplicon reads. The approach is threshold

free, inferring exact variants up to 1 nucleotide of difference using the quality scores distribution in a probability model. After filtering through DADA2, 76.4% of the total reads (mean 64644, min 25135 max 124930) were retained for further analyses. Taxonomic assignation was performed using the function 'assignTaxonomy' against SILVA v.132 (Quast *et al.*, 2012; Yilmaz *et al.*, 2014) through the RDP naive Bayesian classifier method described in Wang *et al.*, (2007). The ASV table was randomly subsampled down to the minimum number of reads per sample using the *rrarefy* function in the *vegan* package (Oksanen *et al.*, 2019). All raw sequences used in this study are publicly available at the European Nucleotide Archive (ERX4135557- ERX4135620). Data treatment and statistical analyses were performed with the R (version 3.3.2) and Rstudio software (version 1.0.44) (R Foundation for Statistical Computing., 2018).

Statistical analyses

We used ANOVA followed by Tukey's Honestly Significant Difference (HSD) test to explore difference between biotic variables (prokaryotic abundance, prokaryotic biomass, contribution of HNA cells, cumulative production) in the different treatments ('Sp SW', 'Sp SW+N', 'Sp BW', 'Sp BW+C', 'Bp SW', 'Bp SW+N', 'Bp BW', 'Bp BW+C'). Paired Wilcoxon signed rank tests were performed to test if the optical properties of DOM in each individual water treatment ('SW', 'SW+N', 'BW', 'BW+C') were different between surface and bathypelagic communities.

Analysis of Alteromonas sequences

We explored in detail the possible species assignment of the two most abundant *Alteromonas* ASVs in our dataset, in order to elucidate whether a single ASV could represent more than one species. To this end, we extracted all the sequences defined as

Alteromonas species from SILVA release 138 (Quast *et al.*, 2012). Sequences were trimmed with cutadapt v1.14 (Martin, 2011) to only keep the V4 and V5 region analyzed in this study. The resultant sequences were aligned with the two ASVs with DECIPHER R package v2.14 (Wright, Erik, 2016), obtaining the nucleotide distances. The results were displayed using a hierarchical clustering heatmap of these distances with the pheatmap R package v1 (Kolde, 2015).

ACKNOWLEDGEMENTS

This work was partially supported by grants DOREMI (CTM2012-34294), HOTMIX (CTM2011-30010/MAR), EcoRARE (CTM2014-60467-JIN), ANIMA (CTM2015-65720-R) and MIAU (RTI2018-101025-B-I00), funded by the Spanish Ministry of Science and also by Grup Generalitat 2017SGR/1568. MS was supported by a Viera y Clavijo contract funded by the ACIISI and the ULPGC. Bioinformatics analyses were performed at the MARBITS platform of the Institut de Ciències del Mar (ICM; http://marbits.icm.csic.es). We thank Clara Ruiz González and three anonymous reviewers for their comments on a previous version of the manuscript.

The authors declare no conflict of interest

REFERENCES

Acinas, S.G., Antón, J., and Rodríguez-Valera, F. (1999) Diversity of free-living and attached bacteria in offshore western Mediterranean waters as depicted by analysis of genes encoding 16S rRNA. *Appl Environ Microbiol* **65**: 514–522.

Acinas, S.G., Sánchez, P., Salazar, G., Cornejo-Castillo, F.M., Sebastián, M., Logares, R., et al. (2019) Metabolic Architecture of the Deep Ocean Microbiome. *bioRxiv*.

Agogué, H., Lamy, D., Neal, P.R., Sogin, M.L., and Herndl, G.J. (2011) Water mass-

specificity of bacterial communities in the North Atlantic revealed by massively parallel sequencing. *Mol Ecol* **20**: 258–274.

Alonso-Sáez, L. and Gasol, J.M. (2007) Seasonal variations in the contributions of different bacterial groups to the uptake of low-molecular-weight compounds in Northwestern Mediterranean coastal waters. *Appl Environ Microbiol* **73**: 3528–3535.

Aparicio, F.L., Nieto-cid, M., Borrull, E., Romero, E., Stedmon, C.A., Sala, M.M., et al. (2015) Microbially-Mediated Fluorescent Organic Matter Transformations in the Deep Ocean . Do the Chemical Precursors Matter ? *Front Mar Sci* **2**: 1–14.

Arístegui, J., Gasol, J.M., Duarte, C.M., and Herndld, G.J. (2009) Microbial oceanography of the dark ocean's pelagic realm. *Limnol Oceanogr* **54**: 1501–1529.

Arrieta, J.M., Mayol, E., Hansman, R.L., Herndl, G.J., Dittmar, T., and Duarte, C.M. (2015) Dilution limits dissolved organic carbon utilization in the deep ocean. *Science (80-)* **348**: 331–333.

Baker, A., Bolton, L., Newson, M., and Spencer, R.G.M. (2008) Spectrophotometric properties of surface water dissolved organic matter in an afforested upland peat catchment. *Hydrol Process* **22**: 2325–2336.

Baltar, F., Arístegui, J., Sintes, E., Van Aken, H.M., Gasol, J.M., and Herndl, G.J. (2009) Prokaryotic extracellular enzymatic activity in relation to biomass production and respiration in the meso- and bathypelagic waters of the (sub)tropical Atlantic. *Environ Microbiol* **11**: 1998–2014.

Bar-On, Y.M., Phillips, R., and Milo, R. (2018) The biomass distribution on Earth. *Proc Natl Acad Sci* **115**: 6506–6511.

Béranger, K., Testor, P., and Crépon, M. (2009) Modelling water mass formation in the gulf of lions (Mediterranean Sea). In *CIESM Workshop Monographs*.

Boutrif, M., Garel, M., Cottrell, M.T., and Tamburini, C. (2011) Assimilation of marine extracellular polymeric substances by deep-sea prokaryotes in the NW Mediterranean Sea. *Environ Microbiol Rep* **3**: 705–709.

Brophy, J.E. and Carlson, D.J. (1989) Production of biologically refractory dissolved organic carbon by natural seawater microbial populations. *Deep Sea Res Part A Oceanogr Res Pap* **36**: 497–507.

Brown, M. V., Philip, G.K., Bunge, J.A., Smith, M.C., Bissett, A., Lauro, F.M., et al. (2009) Microbial community structure in the North Pacific ocean. *ISME J* **3**: 1374–86.

Callahan, B.J., McMurdie, P.J., Rosen, M.J., Han, A.W., Johnson, A.J.A., and Holmes, S.P. (2016) DADA2: High-resolution sample inference from Illumina amplicon data. *Nat Methods* **13**: 581–583.

Cario, A., Oliver, G.C., and Rogers, K.L. (2019) Exploring the Deep Marine Biosphere: Challenges, Innovations, and Opportunities. *Front Earth Sci* **7**:.

Carlson, C.A., Ducklow, H.W., and Michaels, A.F. (1994) Annual flux of dissolved organic carbon from the euphotic zone in the northwestern Sargasso Sea. *Nature* **371**: 405–408.

Carlson, C.A., Giovannoni, S.J., Hansell, D.A., Goldberg, S.J., Parsons, R., and Vergin, K. (2004) Interactions among dissolved organic carbon, microbial processes, and

community structure in the mesopelagic zone of the northwestern Sargasso Sea. *Limnol Oceanogr* **49**: 1073–1083.

Carlson, C.A. and Hansell, D.A. (2015) DOM Sources, Sinks, Reactivity, and Budgets. In *Biogeochemistry of Marine Dissolved Organic Matter*. Elsevier, pp. 65–126.

Carlson, C.A., Hansell, D.A., and Tamburini, C. (2011) DOC Persistence and Its Fate After Export Within the Ocean Interior. In *Microbial carbon pump in the ocean*. Jiao, N., Azam, F., and Sanders, S. (eds). Science/AAAS, pp. 57–59.

Castillo, C.R., Sarmento, H., Álvarez-Salgado, X.A., Gasol, J.M., and Marraséa, C. (2010) Production of chromophoric dissolved organic matter by marine phytoplankton. *Limnol Oceanogr* **55**: 446–454.

Catalá, T.S., Álvarez-Salgado, X.A., Otero, J., Iuculano, F., Companys, B., Horstkotte, B., et al. (2016) Drivers of fluorescent dissolved organic matter in the global epipelagic ocean. *Limnol Oceanogr* **61**: 1101–1119.

Catalá, T.S., Reche, I., Fuentes-Lema, A., Romera-Castillo, C., Nieto-Cid, M., Ortega-Retuerta, E., et al. (2015) Turnover time of fluorescent dissolved organic matter in the dark global ocean. *Nat Commun* **6**: 5986.

Coble, P.G. (1996) Characterization of marine and terrestrial DOM in seawater using excitation-emission matrix spectroscopy. *Mar Chem* **51**: 325–346.

Copin-Montégut, G. and Avril, B. (1993) Vertical distribution and temporal variation of dissolved organic carbon in the North-Western Mediterranean Sea. *Deep Sea Res Part I Oceanogr Res Pap* **40**: 1963–1972.

Cotner, J., Ammerman, J., Peele, E., and Bentzen, E. (1997) Phosphorus-limited bacterioplankton growth in the Sargasso Sea. *Aquat Microb Ecol* **13**: 141–149.

DeLong, E.F., Preston, C.M., Mincer, T.J., Rich, V., Hallam, S.J., Frigaard, N.-U., et al. (2006) Community genomics among stratified microbial assemblages in the ocean's interior. *Science* **311**: 496–503.

Edgcomb, V.P., Taylor, C., Pachiadaki, M.G., Honjo, S., Engstrom, I., and Yakimov, M. (2016) Comparison of Niskin vs. in situ approaches for analysis of gene expression in deep Mediterranean Sea water samples. *Deep Sea Res Part II Top Stud Oceanogr* **129**: 213–222.

Eilers, H., Pernthaler, J., GlÃ¯Â¿Â½ckner, F.O., and Amann, R. (2000) Culturability and In Situ Abundance of Pelagic Bacteria from the North Sea. *Appl Environ Microbiol* **66**: 3044–3051.

Falkowski, P.G., Fenchel, T., and Delong, E.F. (2008) The Microbial Engines That Drive Earth 's Biogeochemical Cycles. *Science (80-)* **320**: 1034–1039.

Ferrera, I., Gasol, J.M., Sebastián, M., Hojerová, E., and Koblížek, M. (2011) Comparison of Growth Rates of Aerobic Anoxygenic Phototrophic Bacteria and Other Bacterioplankton Groups in Coastal Mediterranean Waters. *Appl Environ Microbiol* **77**: 7451–7458.

Garel, M., Bonin, P., Martini, S., Guasco, S., Roumagnac, M., Bhairy, N., et al. (2019) Pressure-Retaining Sampler and High-Pressure Systems to Study Deep-Sea Microbes Under in situ Conditions. *Front Microbiol* **10**:.

Gasol, J.M., Alonso-Sáez, L., Vaqué, D., Baltar, F., Calleja, M.L., Duarte, C.M., and Arístegui, J. (2009) Mesopelagic prokaryotic bulk and single-cell heterotrophic

activity and community composition in the NW Africa–Canary Islands coastal-transition zone. *Prog Oceanogr* **83**: 189–196.

Gasol, J.M. and Del Giorgio, P.A. (2000) Using flow cytometry for counting natural planktonic bacteria and understanding the structure of planktonic bacterial communities. *Sci Mar* **64**: 197–224.

Gasol, J.M. and Moran, X.A.G. (2015) Flow Cytometric Determination of Microbial Abundances and Its Use to Obtain Indices of Community Structure and Relative Activity. *Hydrocarb Lipid Microbiol Protoc - Springer Protoc Handbooks* 1–29.

Ghiglione, J.-F., Galand, P.E., Pommier, T., Pedros-Alio, C., Maas, E.W., Bakker, K., et al. (2012) Pole-to-pole biogeography of surface and deep marine bacterial communities. *Proc Natl Acad Sci* **109**: 17633–17638.

del Giorgio, P.A., Condon, R., Bouvier, T., Longnecker, K., Bouvier, C., Sherr, E., and Gasol, J.M. (2011) Coherent patterns in bacterial growth, growth efficiency, and leucine metabolism along a northeastern Pacific inshore-offshore transect. *Limnol Oceanogr* **56**: 1–16.

Gómez-Consarnau, L., Needham, D.M., Weber, P.K., Fuhrman, J.A., and Mayali, X. (2019) Influence of Light on Particulate Organic Matter Utilization by Attached and Free-Living Marine Bacteria. *Front Microbiol* **10**:.

Grossart, H. and Gust, G. (2009) Hydrostatic pressure affects physiology and community structure of marine bacteria during settling to 4000 m: an experimental approach. *Mar Ecol Prog Ser* **390**: 97–104.

Guieysse, B. and Wuertz, S. (2012) Metabolically versatile large-genome prokaryotes. *Curr Opin Biotechnol* **23**: 467–473.

Gundersen, K., Heldal, M., Norland, S., Purdie, D.A.A.D.A., and Knap, A.H.H.A.H. (2002) Elemental C, N, and P cell content of individual bacteria collected at the Bermuda Atlantic Time-series Study (BATS) site. *Limnol Oceanogr* **47**: 1525–1530.

Hansell, D.A. (2013) Recalcitrant Dissolved Organic Carbon Fractions. *Ann Rev Mar Sci* **5**: 421–445.

Hansell, D.A. and Carlson, C.A. (2001) Biogeochemistry of total organic carbon and nitrogen in the Sargasso Sea: control by convective overturn. *Deep Sea Res Part II Top Stud Oceanogr* **48**: 1649–1667.

Hansen, H.P. and Koroleff, F. (2007) Determination of nutrients. In *Methods of Seawater Analysis*. Weinheim, Germany: Wiley-VCH Verlag GmbH, pp. 159–228.

Helms, J.R., Stubbins, A., Ritchie, J.D., Minor, E.C., Kieber, D.J., and Mopper, K. (2008) Absorption spectral slopes and slope ratios as indicators of molecular weight, source, and photobleaching of chromophoric dissolved organic matter. *Limnol Oceanogr* **53**: 955–969.

Herndl, G.J. and Reinthaler, T. (2013) Microbial control of the dark end of the biological pump. *Nat Geosci* **6**: 718–724.

Hopkinson, C.S. and Vallino, J.J. (2005) Efficient export of carbon to the deep ocean through dissolved organic matter. *Nature* **433**: 142–145.

Hoppe, H. (2003) Phosphatase activity in the sea. *Hydrobiologia* 187–200.

Hoppe, H. (1983) Significance of exoenzymatic activities in the ecology of brackish water: measurements by means of methylumbelliferyl-substrates. *Mar Ecol Prog Ser* **11**: 299–308.

Hoppe, H. and Ullrich, S. (1999) Profiles of ectoenzymes in the Indian Ocean: phenomena of phosphatase activity in the mesopelagic zone. *Aquat Microb Ecol* **19**: 139–148.

Ivars-Martinez, E., Martin-Cuadrado, A.B., D'Auria, G., Mira, A., Ferriera, S., Johnson, J., et al. (2008) Comparative genomics of two ecotypes of the marine planktonic copiotroph Alteromonas macleodii suggests alternative lifestyles associated with different kinds of particulate organic matter. *ISME J* **2**: 1194–1212.

Jiao, N., Herndl, G.J., Hansell, D. a, Benner, R., Kattner, G., Wilhelm, S.W., et al. (2010) Microbial production of recalcitrant dissolved organic matter: long-term carbon storage in the global ocean. *Nat Rev Microbiol* **8**: 593–9.

Jørgensen, L., Stedmon, C.A., Granskog, M.A., and Middelboe, M. (2014) Tracing the long-term microbial production of recalcitrant fluorescent dissolved organic matter in seawater. *Geophys Res Lett* **41**: 2481–2488.

Jørgensen, L., Stedmon, C.A., Kragh, T., Markager, S., Middelboe, M., and Søndergaard, M. (2011) Global trends in the fluorescence characteristics and distribution of marine dissolved organic matter. *Mar Chem* **126**: 139–148.

Kirchman, D., Dittel, A., Findlay, S., and Fischer, D. (2004) Changes in bacterial activity and community structure in response to dissolved organic matter in the Hudson River, New York. *Aquat Microb Ecol* **35**: 243–257.

Kirchman, D., K'nees, E., and Hodson, R. (1985) Leucine incorporation and its potential as a measure of protein synthesis by bacteria in natural aquatic systems. *Appl Environ Microbiol* **49**: 599–607.

Kolde, R. (2015) pheatmap : Pretty Heatmaps. *R Packag version 108*.

Kolter, R. (1993) The Stationary Phase of the Bacterial Life Cycle. *Annu Rev Microbiol* **47**: 855–874.

De La Fuente, P., Marrasé, C., Canepa, A., Antón Álvarez-Salgado, X., Gasser, M., Fajar, N.M., et al. (2014) Does a general relationship exist between fluorescent dissolved organic matter and microbial respiration?—The case of the dark equatorial Atlantic Ocean. *Deep Sea Res Part I Oceanogr Res Pap* **89**: 44–55.

Lauro, F.M. and Bartlett, D.H. (2008) Prokaryotic lifestyles in deep sea habitats. *Extremophiles* **12**: 15–25.

Lawaetz, A.J. and Stedmon, C.A. (2009) Fluorescence Intensity Calibration Using the Raman Scatter Peak of Water. *Appl Spectrosc* **63**: 936–940.

Li, J., Wei, B., Wang, J., Liu, Y., Dasgupta, S., Zhang, L., and Fang, J. (2015) Variation in abundance and community structure of particle-attached and free-living bacteria in the South China Sea. *Deep Sea Res Part II Top Stud Oceanogr* **122**: 64–73.

Lopez-Lopez, A., Bartual, S.G., Stal, L., Onyshchenko, O., and Rodriguez-Valera, F. (2005) Genetic analysis of housekeeping genes reveals a deep-sea ecotype of Alteromonas macleodii in the Mediterranean Sea. *Environ Microbiol* **7**: 649–659.

López-Pérez, M., Gonzaga, A., Martin-Cuadrado, A.-B., Onyshchenko, O., Ghavidel, A., Ghai, R., and Rodriguez-Valera, F. (2012) Genomes of surface isolates of

Alteromonas macleodii: the life of a widespread marine opportunistic copiotroph. *Sci Rep* **2**: 696.

Luna, G.M., Chiggiato, J., Quero, G.M., Schroeder, K., Bongiorni, L., Kalenitchenko, D., and Galand, P.E. (2016) Dense water plumes modulate richness and productivity of deep sea microbes. *Environ Microbiol* **18**: 4537–4548.

MacDonell, M.T. and Hood, M.A. (1982) Isolation and Characterization of Ultramicrobacteria from a Gulf Coast Estuary. *Appl Environ Microbiol* **43**: 566–571.

Martin, M. (2011) Cutadapt removes adapter sequences from high-throughput sequencing reads. *EMBnet.journal* **17**: 10.

Martínez-Pérez, A.M., Nieto-Cid, M., Osterholz, H., Catalá, T.S., Reche, I., Dittmar, T., and Álvarez-Salgado, X.A. (2017) Linking optical and molecular signatures of dissolved organic matter in the Mediterranean Sea. *Sci Rep* **7**: 3436.

McCarren, J., Becker, J.W., Repeta, D.J., Shi, Y., Young, C.R., Malmstrom, R.R., et al. (2010) Microbial community transcriptomes reveal microbes and metabolic pathways associated with dissolved organic matter turnover in the sea. *Proc Natl Acad Sci* **107**: 16420–16427.

Mestre, M., Borrull, E., Sala, M.M., and Gasol, J.M. (2017) Patterns of bacterial diversity in the marine planktonic particulate matter continuum. *ISME J* **11**: 999–1010.

Mestre, M., Ruiz-González, C., Logares, R., Duarte, C.M., Gasol, J.M., and Sala, M.M. (2018) Sinking particles promote vertical connectivity in the ocean microbiome. *Proc Natl Acad Sci U S A* **115**: E6799–E6807.

Mills, M.M., Moore, C.M., Langlois, R., Milne, A., Achterberg, E., Nachtigall, K., et al. (2008) Nitrogen and phosphorus co-limitation of bacterial productivity and growth in the oligotrophic subtropical North Atlantic. *Limnol Oceanogr* **53**: 824–834.

Nelson, C.E. and Carlson, C.A. (2012) Tracking differential incorporation of dissolved organic carbon types among diverse lineages of Sargasso Sea bacterioplankton. *Environ Microbiol* **14**: 1500–16.

Novitsky, J.A. and Morita, R.Y. (1976) Morphological characterization of small cells resulting from nutrient starvation of a psychrophilic marine vibrio. *Appl Environ Microbiol* **32**: 617–622.

Novitsky, J.A. and Morita, R.Y. (1977) Survival of a psychrophilic marine vibrio under long term nutrient starvation. *Appl Environ Microbiol* **33**: 635–641.

Ogawa, H., Amagai, Y., Koike, I., Kaiser, K., and Benner, R. (2001) Production of refractory dissolved organic matter by bacteria. *Science (80-)* **292**: 917–20.

Oksanen, J., Blanchet, F.G., Friendly, M., Kindt, R., Legendre, P., Mcglinn, D., et al. (2019) Package "vegan" Title Community Ecology Package. *Community Ecol Packag*.

Ortega-Retuerta, E., Frazer, T.K., Duarte, C.M., Ruiz-Halpern, S., Tovar-Sánchez, A., Arrieta, J.M., and Rechea, I. (2009) Biogeneration of chromophoric dissolved organic matter by bacteria and krill in the Southern Ocean. *Limnol Oceanogr* **54**: 1941–1950.

Osterholz, H., Niggemann, J., Giebel, H.-A., Simon, M., and Dittmar, T. (2015)

944 Inefficient microbial production of refractory dissolved organic matter in the
945 ocean. *Nat Commun* **6**: 7422.

946 Pedler, B.E., Aluwihare, L.I., and Azam, F. (2014) Single bacterial strain capable of
947 significant contribution to carbon cycling in the surface ocean. *Proc Natl Acad Sci*
948 **111**: 7202–7207.

949 Pinhassi, J., Gómez-Consarnau, L., Alonso-Sáez, L., Sala, M.M., Vidal, M., Pedrós-
950 Alio, C., and Gasol, J.M. (2006) Seasonal changes in bacterioplankton nutrient
951 limitation and their effects on bacterial community composition in the NW
952 Mediterranean Sea. *Aquat Microb Ecol* **44**: 241–252.

953 Pommier, T., Neal, P., Gasol, J., Coll, M., Acinas, S., and Pedrós-Alió, C. (2010)
954 Spatial patterns of bacterial richness and evenness in the NW Mediterranean Sea
955 explored by pyrosequencing of the 16S rRNA. *Aquat Microb Ecol* **61**: 221–233.

956 Quast, C., Pruesse, E., Yilmaz, P., Gerken, J., Schweer, T., Yarza, P., et al. (2012) The
957 SILVA ribosomal RNA gene database project: improved data processing and web-
958 based tools. *Nucleic Acids Res* **41**: D590–D596.

959 R Foundation for Statistical Computing. (2018) R: a Language and Environment for
960 Statistical Computing.

961 Romera-Castillo, C., Álvarez-Salgado, X.A., Galí, M., Gasol, J.M., and Marrasé, C.
962 (2013) Combined effect of light exposure and microbial activity on distinct
963 dissolved organic matter pools. A seasonal field study in an oligotrophic coastal
964 system (Blanes Bay, NW Mediterranean). *Mar Chem* **148**: 44–51.

965 Romera-Castillo, C., Sarmento, H., Álvarez-Salgado, X.A., Gasol, J.M., and Marrasé,
966 C. (2011) Net Production and Consumption of Fluorescent Colored Dissolved
967 Organic Matter by Natural Bacterial Assemblages Growing on Marine
968 Phytoplankton Exudates. *Appl Environ Microbiol* **77**: 7490–7498.

969 Romera-Castillo, C., Álvarez, M., Pelegrí, J.L., Hansell, D.A., and Álvarez-Salgado,
970 X.A. (2019) Net Additions of Recalcitrant Dissolved Organic Carbon in the Deep
971 Atlantic Ocean. *Global Biogeochem Cycles* **33**: 1162–1173.

972 Sala, M.M., Aparicio, F.L., Balagué, V., Boras, J.A., Borrull, E., Cardelús, C., et al.
973 (2016) Contrasting effects of ocean acidification on the microbial food web under
974 different trophic conditions. *ICES J Mar Sci* **73**: 670–679.

975 Salazar, G., Cornejo-Castillo, F.M., Benítez-Barrios, V., Fraile-Nuez, E., Álvarez-
976 Salgado, X.A., Duarte, C.M., et al. (2016) Global diversity and biogeography of
977 deep-sea pelagic prokaryotes. *ISME J* **10**: 596–608.

978 Salazar, G., Cornejo-Castillo, F.M., Borrull, E., Díez-Vives, C., Lara, E., Vaqué, D., et
979 al. (2015) Particle-association lifestyle is a phylogenetically conserved trait in
980 bathypelagic prokaryotes. *Mol Ecol* **24**: 5692–5706.

981 Sánchez, O., Koblížek, M., Gasol, J.M., and Ferrera, I. (2017) Effects of grazing,
982 phosphorus and light on the growth rates of major bacterioplankton taxa in the
983 coastal NW Mediterranean. *Environ Microbiol Rep* **9**: 300–309.

984 Santinelli, C. (2015) DOC in the Mediterranean Sea. In *Biogeochemistry of Marine*
985 *Dissolved Organic Matter*. Elsevier, pp. 579–608.

986 Schäfer, H., Servais, P., and Muyzer, G. (2000) Successional changes in the genetic
987 diversity of a marine bacterial assemblage during confinement. *Arch Microbiol*

173: 138–145.

Sebastián, M., Auguet, J.-C., Restrepo-Ortiz, C.X., Sala, M.M., Marrasé, C., and Gasol, J.M. (2018) Deep ocean prokaryotic communities are remarkably malleable when facing long-term starvation. *Environ Microbiol* **20**: 713–723.

Sebastián, M., Estrany, M., Ruiz-González, C., Forn, I., Sala, M.M., Gasol, J.M., and Marrasé, C. (2019) High Growth Potential of Long-Term Starved Deep Ocean Opportunistic Heterotrophic Bacteria. *Front Microbiol* **10**:.

Severin, T., Sauret, C., Boutrif, M., Duhaut, T., Kessouri, F., Oriol, L., et al. (2016) Impact of an intense water column mixing (0-1500 m) on prokaryotic diversity and activities during an open-ocean convection event in the NW Mediterranean Sea. *Environ Microbiol* **18**: 4378–4390.

Shen, Y. and Benner, R. (2018) Mixing it up in the ocean carbon cycle and the removal of refractory dissolved organic carbon. *Sci Rep* **8**: 2542.

Shen, Y. and Benner, R. (2020) Molecular properties are a primary control on the microbial utilization of dissolved organic matter in the ocean. *Limnol Oceanogr* **65**: 1061–1071.

Simon, M. and Azam, F. (1989) Protein content and protein synthesis rates of planktonic marine bacteria. *Mar Ecol Prog Ser* **51**: 201–213.

Smith, D. and Azam, F. (1992) A simple, economical method for measuring bacterial protein synthesis rates in seawater using. *Mar Microb food webs* **6**: 107–114.

Smith, K.L., Ruhl, H.A., Huffard, C.L., Messié, M., and Kahru, M. (2018) Episodic organic carbon fluxes from surface ocean to abyssal depths during long-term monitoring in NE Pacific. *Proc Natl Acad Sci* **115**: 12235–12240.

Sogin, M.L., Morrison, H.G., Huber, J.A., Welch, D.M., Huse, S.M., Neal, P.R., et al. (2006) Microbial diversity in the deep sea and the underexplored "rare biosphere." *Proc Natl Acad Sci* **103**: 12115–12120.

Sunagawa, S., Coelho, L.P., Chaffron, S., Kultima, J.R., Labadie, K., Salazar, G., et al. (2015) Structure and function of the global ocean microbiome. *Science (80-)* **348**: 1261359-12c61359.

Tamburini, C., Boutrif, M., Garel, M., Colwell, R.R., and Deming, J.W. (2013) Prokaryotic responses to hydrostatic pressure in the ocean - a review. *Environ Microbiol* **15**: 1262–1274.

Tamburini, C., Canals, M., Durrieu de Madron, X., Houpert, L., Lefèvre, D., Martini, S., et al. (2013) Deep-Sea Bioluminescence Blooms after Dense Water Formation at the Ocean Surface. *PLoS One* **8**: e67523.

Thingstad, T.F., HagstrÖm, Å., and Rassoulzadegan, F. (1997) Accumulation of degradable DOC in surface waters: Is it caused by a malfunctioning microbialloop? *Limnol Oceanogr* **42**: 398–404.

Treusch, A.H., Vergin, K.L., Finlay, L.A., Donatz, M.G., Burton, R.M., Carlson, C.A., and Giovannoni, S.J. (2009) Seasonality and vertical structure of microbial communities in an ocean gyre. *ISME J* **3**: 1148–1163.

VanInsberghe, D., Arevalo, P., Chien, D., and Polz, M.F. (2020) How can microbial population genomics inform community ecology? *Philos Trans R Soc B Biol Sci* **375**: 20190253.

1032 Vezzi, A. (2005) Life at Depth: Photobacterium profundum Genome Sequence and
1033 Expression Analysis. *Science (80-)* **307**: 1459–1461.

1034 Van Wambeke, F., Catala, P., Pujo-Pay, M., and Lebaron, P. (2011) Vertical and
1035 longitudinal gradients in HNA-LNA cell abundances and cytometric characteristics
1036 in the Mediterranean Sea. *Biogeosciences* **8**: 1853–1863.

1037 Wang, Q., Garrity, G.M., Tiedje, J.M., and Cole, J.R. (2007) Naïve Bayesian Classifier
1038 for Rapid Assignment of rRNA Sequences into the New Bacterial Taxonomy. *Appl*
1039 *Environ Microbiol* **73**: 5261–5267.

1040 Whitman, W.B., Coleman, D.C., and Wiebe, W.J. (1998) Prokaryotes: The unseen
1041 majority. *Proc Natl Acad Sci* **95**: 6578–6583.

1042 Wright, Erik, S. (2016) Using DECIPHER v2.0 to Analyze Big Biological Sequence
1043 Data in R. *R J* **8**: 352.

1044 Yamashita, Y. and Tanoue, E. (2003) Chemical characterization of protein-like
1045 fluorophores in DOM in relation to aromatic amino acids. *Mar Chem* **82**: 255–271.

1046 Yamashita, Y. and Tanoue, E. (2008) Production of bio-refractory fluorescent dissolved
1047 organic matter in the ocean interior. *Nat Geosci* **1**: 579–582.

1048 Yilmaz, P., Parfrey, L.W., Yarza, P., Gerken, J., Pruesse, E., Quast, C., et al. (2014) The
1049 SILVA and "All-species Living Tree Project (LTP)" taxonomic frameworks.
1050 *Nucleic Acids Res* **42**: D643–D648.

1051

1052

1053 **FIGURE LEGENDS**

1054 **Figure 1**. Abundance (a), cell size (b) and heterotrophic production (c) of surface
1055 prokaryotes (Sp, open circles) and bathypelagic prokaryotes (Bp, filled circles) inoculated
1056 in surface waters (SW, left panel), surface waters with nutrients (SW+N, second panel),
1057 and bathypelagic waters (BW, third panel). The asterisk represents the moment when
1058 mixed sources of organic carbon were added to a subsample of the bathypelagic waters
1059 treatment (see methods). The small panel on the right represents how this carbon-enriched
1060 BW treatment evolved (BW+C). Note the change in scale in the BW+C for cell
1061 abundance. Each data point represents the average of two replicates and error bars
1062 represent the range of values.

1063

1064 **Figure 2**. Taxonomic changes in the different treatments along the transplant experiment.

Initial: community at the moment of sampling. Inoculum: starting community (after prefiltration through a 0.8µm filter, collection of cells onto a 0.2µm filter and resuspension). SW: surface waters, SW+N: surface waters with added nutrients, BW: bathypelagic waters, BW+C: bathypelagic waters with added labile carbon.

Figure 3. Boxplot of a) Shannon and Evenness of surface and bathypelagic communities over the course of the experiment. b) the number of taxa (ASV) that were rare in the starting community but represented more than 5% of the community each of the time-points of the experiment, here considered as opportunistic taxa. Sp: surface prokaryotes, Bp: bathypelagic prokaryotes, SW: surface waters, SW+N: surface waters with added nutrients, BW: bathypelagic waters.

Figure 4. Temporal dynamics of specific enzymatic activities of surface prokaryotes (Sp, open circles) and bathypelagic prokaryotes (Bp, filled circles) inoculated in surface waters (SW, left panel), surface waters with nutrients (SW+N, second panel), and bathypelagic waters (BW, third panel). The asterisk represents the moment when mixed sources of carbon were added to a subsample (half of the remaining volume) of the bathypelagic waters treatment (see methods). The small panel on the right represents how this carbon-enriched BW treatment evolved (BW+C). Each data point represents the average of two biological replicates and error bars represent the range of values.

Figure 5. Characterization of the dissolved organic matter (DOM) **a)** fluorescent DOM: Humic-like substances (C peak, upper panel), protein-like substances (T peak, middle panel) and C/T peak ratio (an indication of the amount of recalcitrant versus labile

material, lower panel). Each data point represents the average of two biological replicates (with four technical replicates each) and the error bars represent the range of values. **b)** Percent change in the spectral slope of the chromophoric DOM in the 275-295 nm wavelength range from the beginning to the end of the experiment. A decrease in the slope is indicative of an increase in aromaticity. Sp: surface prokaryotes, Bp: bathypelagic prokaryotes, SW: surface waters, SW+N: surface waters with added nutrients, BW: bathypelagic waters, BW+C: bathypelagic waters with added carbon.

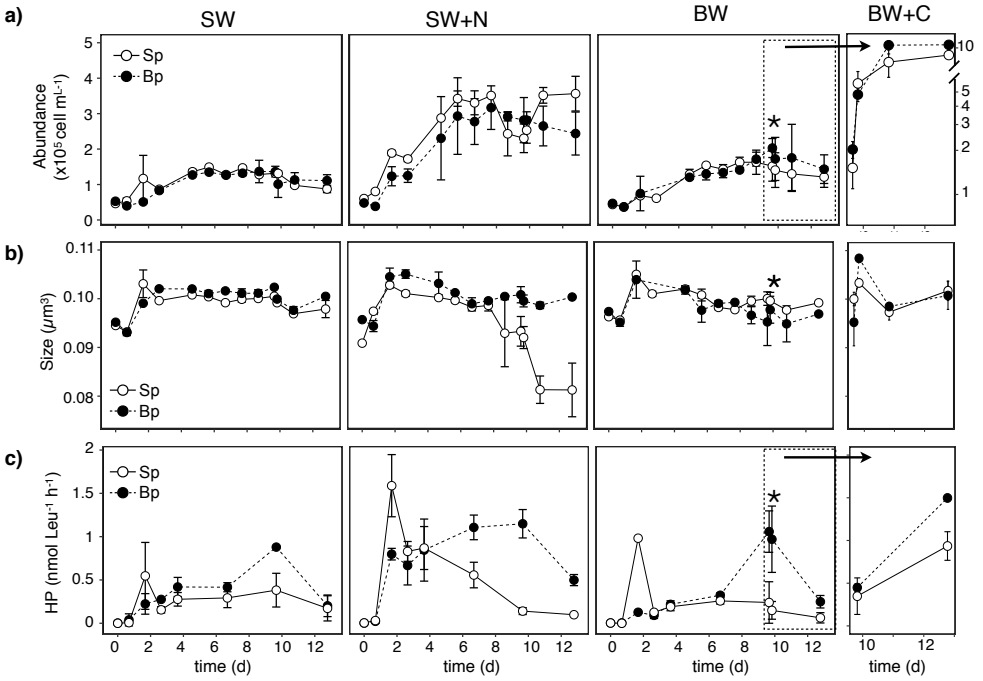
a)
SW
SW+N
BW
BW+C
Sp
Bp
Abundance (x10⁵ cell ml⁻¹)
b)
Size (μm³)
c)
HP (nmol Leu⁻¹ h⁻¹)
time (d)

Figure 1

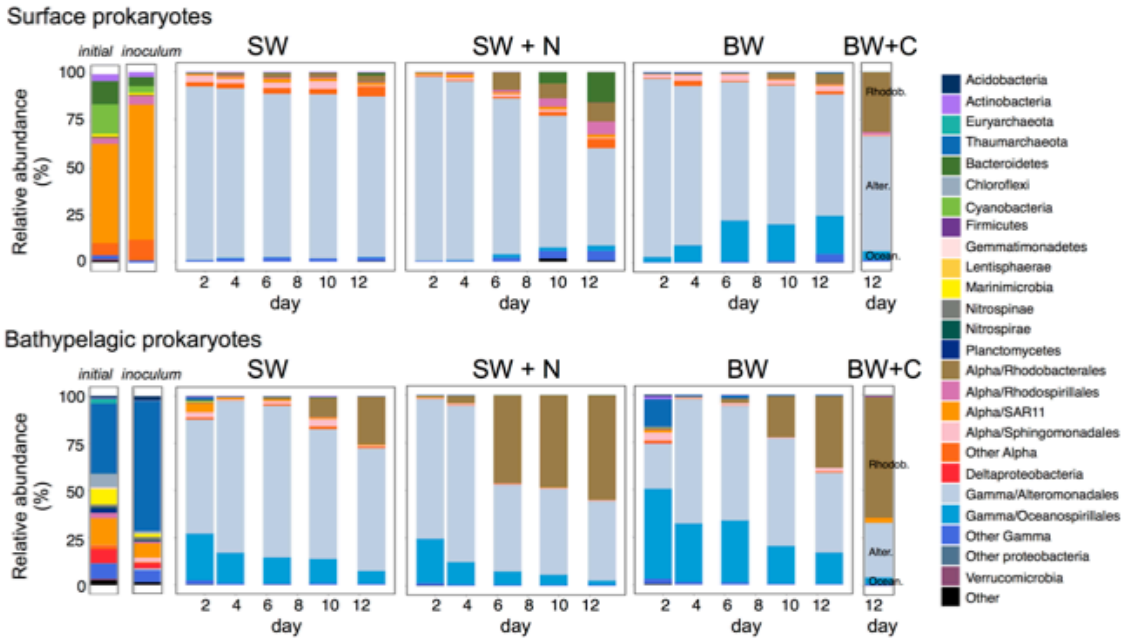
Surface prokaryotes
initial
inoculum
SW
SW + N
BW
BW+C
Relative abundance (%)
100
75
50
25
0
2 4 6 8 10 12
day
Rhodob.
Alter.
Ocean.
Bathypelagic prokaryotes
Acidobacteria
Actinobacteria
Euryarchaeota
Thaumarchaeota
Bacteroidetes
Chloroflexi
Cyanobacteria
Firmicutes
Gemmatimonadetes
Lentisphaerae
Marinimicrobia
Nitrospinae
Nitrospirae
Planctomycetes
Alpha/Rhodobacterales
Alpha/Rhodospirillales
Alpha/SAR11
Alpha/Sphingomonadales
Other Alpha
Deltaproteobacteria
Gamma/Alteromonadales
Gamma/Oceanospirillales
Other Gamma
Other proteobacteria
Verrucomicrobia
Other

Figure 2

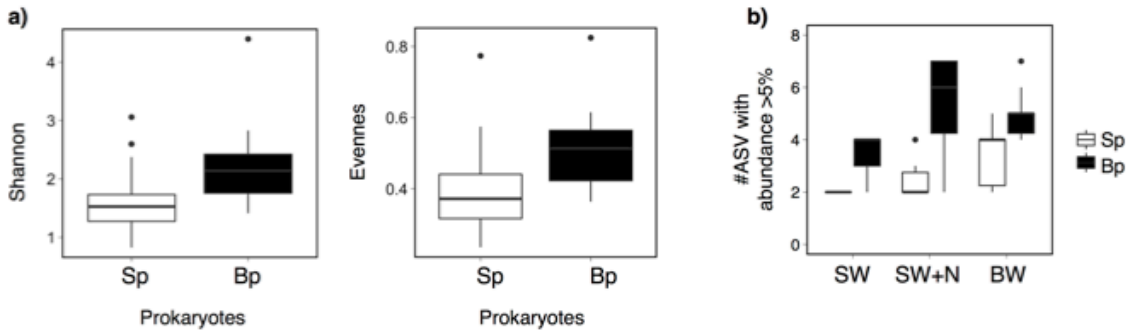
a)
Shannon
Sp
Bp
Prokaryotes
Evennes
Sp
Bp
Prokaryotes
b)
#ASV with abundance >5%
SW
SW+N
BW
Sp
Bp

Figure 3

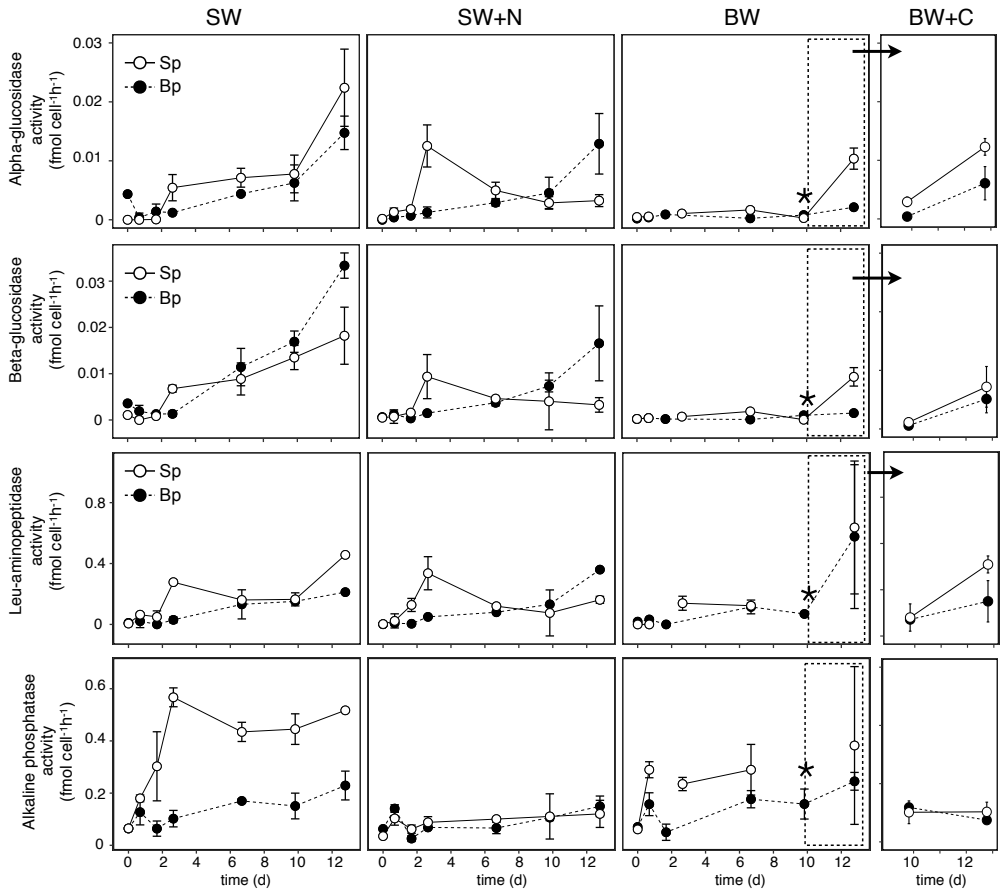
SW
SW+N
BW
BW+C
Sp
Bp
Alpha-glucosidase activity (fmol cell⁻¹h⁻¹)
Beta-glucosidase activity (fmol cell⁻¹h⁻¹)
Leu-aminopeptidase activity (fmol cell⁻¹h⁻¹)
Alkaline phosphatase activity (fmol cell⁻¹h⁻¹)
time (d)

Figure 4

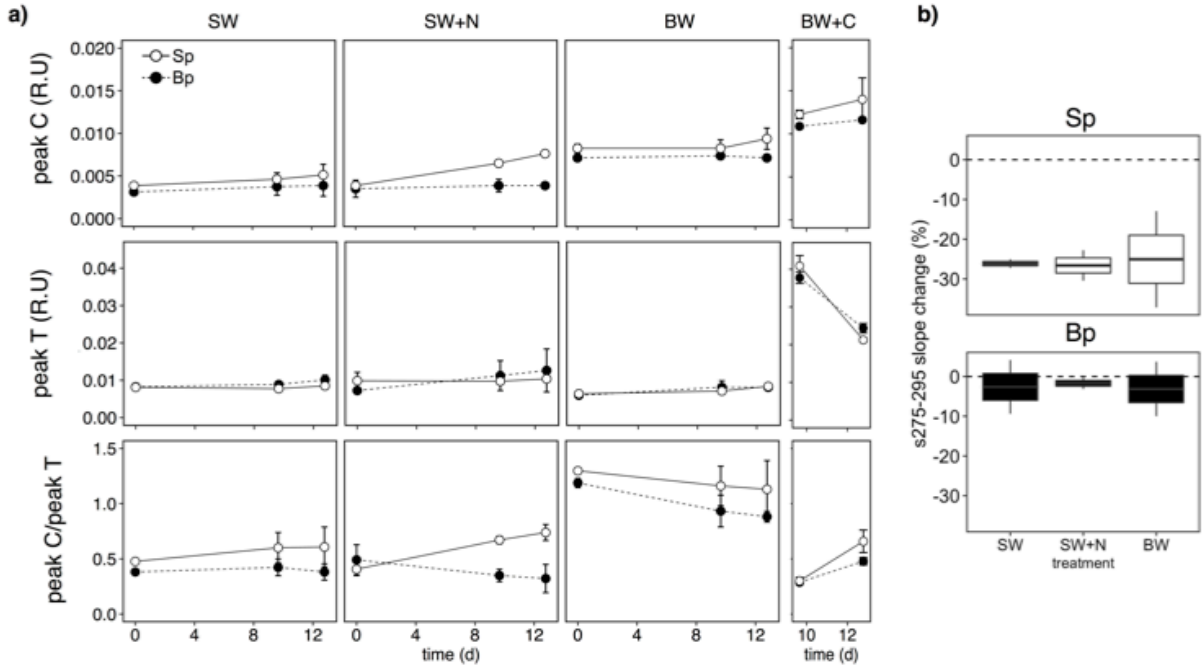
a)
SW
SW+N
BW
BW+C
Sp
Bp
peak C (R.U)
peak T (R.U)
peak C/peak T
time (d)
b)
Sp
Bp
s275-295 slope change (%)
SW
SW+N
BW
treatment

Figure 5

1117

Table 1. Inorganic nutrients and total organic carbon concentrations at the beginning of the experiment. SW: Surface water, SW +N: Surface water enriched with N and P, BW: Bathypelagic water. BW+C: Bathypelagic water with added carbon (see methods for details). Values in parenthesis represent the range of values.

	Nitrate (µM)	**Phosphate (µM)**	**TOC (µM)**
SW	0.4 (0.3)	0.05 (0.01)	78 (2.3)
SW + N	13 (0.4)	0.5 (0.03)	78 (3.8)
BW	9.7 (0.7)	0.4 (0.06)	47 (3.9)
BW + C	--	--	63.8 (4.3)

1118

1119

Table 2. Comparison of the biological properties among the treatments. Values for prokaryotic abundance (PA), biomass and %HNA (proportion of high nucleic acid prokaryotes) represent the average of the values once saturation in cell abundance was reached (from day 6 till the end of the experiment). Cumulative heterotrophic production (PHP) is also shown (average and range of values for the two replicates). Different letters in each row represent values that are significantly different from each other (as analyzed by ANOVA followed by Tukey's Honestly Significant Difference (HSD) test, $p<0.01$). Significant differences between surface and bathypelagic communities within each water treatment are highlighted in bold for clarity.

	SW		**SW+N**		**BW**		**BW+C**	
	Sp	Bp	Sp	Bp	Sp	Bp	Sp	Bp
PA ($x10^5$ cells mL^{-1})	1.2^a	1.2^a	3.0^b	2.8^b	1.4^a	1.6^a	7.6^c	8.6^c
Biomass ($\mu gC\ L^{-1}$)	2.83^a	2.89^a	6.42^b	6.65^b	3.41^a	3.78^a	18.1^c	20.7^c
%HNA	80^a	87^a	**59**^{b}	**94**^{c}	93^d	92^d	99^e	99^e
Cum. PHP ($\mu gC\ L^{-1}$)	131 ± 15^a	202 ± 12^a	**211 ±24**^{a}	**394 ±12**^{b}	111 ± 20^a	203 ± 6^a	**208 ±26**^{a}	**336 ±12**^{b}